METAMATERIAL-BASED HIGHLY DIRECTIVE ANTENNA: APPLICATION IN A MONOCHROMATIC WAVE RADAR FOR A CONTACTLESS MEASUREMENT OF THE BREATHING ACTIVITY

Riad Yahiaoui[1, *], Régis Chantalat[2], Nicolas Chevalier[2], Marc Jouvet[1], and Michèle Lalande[1]

[1]XLIM, Université de Limoges, CNRS, UMR 6172, 7 rue Jules Vallès, Brive 19100, France

[2]CISTEME, Parc ESTER 1, 12 rue Gémini, Limoges 87000, France

Abstract—We report the numerical and experimental investigation of a highly directive Fabry-Pérot (FP) cavity antenna based on a metamaterial, operating in the microwave regime. Numerical simulations using finite element method and reflection-transmission microwave measurements have been performed and a good quantitative agreement has been observed. Measured return losses and radiations patterns done in an anechoic chamber agree very well with the simulated ones. The potential application of the proposed FP cavity antenna in a non-contact breathing sensor is proposed and evaluated. Experimental record and frequency spectrum for respiratory movements of human-being (voluntary under test) are presented. The low cost and simple fabrication process of the proposed FP cavity antenna make it very promising for its integration in modern telecommunication systems.

1. INTRODUCTION

For long time, radar-systems were restricted to military sector. Recently, large number of scientific research paved the way to many interesting applications, particularly in the field of biomedical sensing [1, 2]. Due to their ability for contactless measurement, radars are considered as a very promising solution to implement systems that allow monitoring vital parameters of patients in hospitals (respiratory

* Corresponding author: Riad Yahiaoui (riad.yahiaoui@unilim.fr).

movement, cardiopulmonary activity, and so on). There are other cases whose monitoring and detection can take advantage by the use of radar technologies, such as: anti-criminal detachments, and rescue services to detect survivors during earthquakes and other disasters. For this latter case, the system must be able to detect both physiological signatures and the position of the target. It is also possible to prevent the sudden infant death syndrome (SIDS) and the cases of sleep apnea. Another application is the monitoring of vital functions of the fetus during critical pregnancy.

Most existing measurement techniques require wearing devices, which turns out to be very invasive for patients. This problem becomes very critical when wearing these devices is virtually impossible (e.g., monitoring burned patients). As an alternative to overcome these drawbacks, we propose in this work a contactless monitoring system operating at 5.8 GHz to measure the breathing activity of human being.

The antenna selection is a key parameter in determining the spatial sensitivity of the sensor. In this present work, dealing with a point-to-point communication (the position of the transmitting antenna and the target are known a priori), and pushed by the necessity to miniaturize the system, we focused on directive planar antennas technology, suitable to increase both the scope of the radio communications links and the flow of the transmissions. Several techniques can be used in order to enhance the directivity of antennas, such as lenses antennas, and printed antennas array, but the feeding mechanism of the array leads to a significantly loss in efficiency. Another way to achieve directive antennas is to place a source between two reflectors to form the so-called: Fabry-Pérot (FP) resonant cavity antenna, as introduced for the first time by Trentini in the 1950's [3]. In recent years, this class of antennas has received renewed interest particularly with the development of metallo-dielectric periodic structures, and they have been studied as reflex-cavity antennas for their directive emissions [4–10]. First, a metamaterial-based periodic structure (metasurface) is presented. The investigated metasurface will be used as a Partially Reflecting Surface (PRS) in a Fabry-Pérot cavity antenna in order to enhance the directivity of printed patch antenna. The proposed FP cavity antenna is integrated in a contactless sensor to evaluate the respiration. Experimental record and frequency spectrum for respiratory movements of human-being are presented.

2. DESIGN, FABRICATION AND EXPERIMENTAL CHARACTERIZATION OF THE PROPOSED METASURFACE

The elementary cell of the proposed metasurface is shown in Fig. 1(a). It consists of $35\,\mu m$ thick metallic (copper) patterns printed on the top face of $1.6\,mm$ thick epoxy substrate ($\varepsilon_r = 4.7$, $\tan(\delta) = 0.019$), with the relevant geometrical dimensions: $a = b = 28\,mm$, $c = 26\,mm$, $d = 5\,mm$. Using the full wave electromagnetic simulator HFSS based on the finite element method, we performed simulations in order to predict the spectral response of the structure. The sample is illuminated by TM-polarized plane wave at normal incidence with only one layer along the direction of propagation k. The proposed metasurface acts like a spatial filter. Once exposed to an electromagnetic radiation, some frequency bands are transmitted and some are reflected. Its operating principle can be explained by the phenomenon of resonance. Upon interacting with an incident plane-wave, the elements of the periodic surface resonate at frequencies where the effective length of the elements is a multiple of the resonance length $\lambda/2$. The electromagnetic behavior of the proposed metasurface is entirely determined by the geometry of the elementary cell and the properties of the dielectric
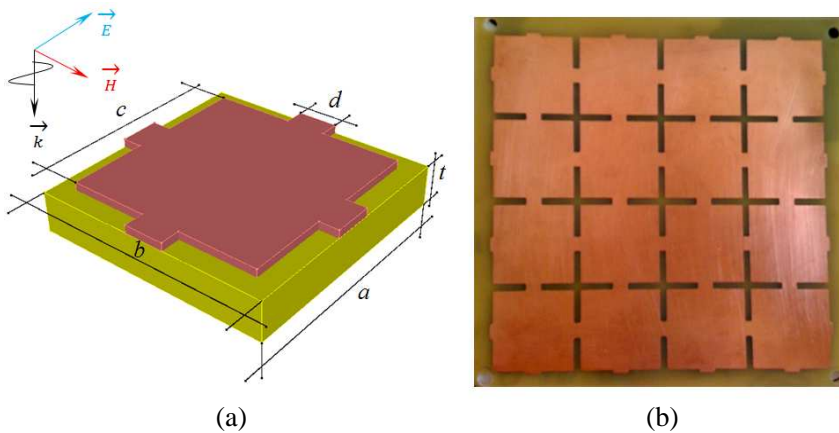

(a)   (b)

Figure 1. (a) Elementary cell of our proposed metasurface acting as partially reflecting surface, with the relevant geometrical dimensions: $a = b = 28\,mm$, $c = 26\,mm$, $d = 5\,mm$ and $t = 1.6\,mm$. The appropriate polarization of the electric E and magnetic H fields is also shown. (b) Image of the fabricated prototype using standard optical lithography.

substrate ε_r and $\tan\delta$. Due to the symmetric geometry of the elementary cell of the metasurface, which combines both continues wires along E and H fields and square patches, the spectral response remains insensitive in the case of an incident TE-polarized plane wave (in other words, the structure supports a double polarization TE and TM). To confirm the numerical predictions, we have fabricated an experimental prototype composed of 4×4 elementary cells using standard optical lithography (see Fig. 1(b)). Measurements have been done in an anechoic chamber using a vector network analyzer. Two broadband FLANN® horn antennas working in the 2–18 GHz frequency band are used as emitter and receiver. In the transmission measurements, the incident plane waves are normal to the sample surface and the transmitted intensity is normalized with respect to transmission in free space between the two horn antennas. Similarly, the reflection coefficient is normalized using a sheet of copper as reflecting mirror.

The magnitudes and phases of transmission T and reflection R coefficients are plotted in Fig. 2(a) and Fig. 2(b), respectively for the 3–7 GHz frequency band. A good quantitative agreement between simulation and experiment is reported. One can observe a band-pass behavior centred around 4.25 GHz with a FWHM (full width at half maximum) bandwidth in the transmission spectrum of about 0.8 GHz. Although there are minor differences in amplitude, bandwidth, and a frequency shift of the resonance due to manufacturing imperfections, the spectral responses obtained in measurement confirm very well the trend calculated from simulation. Note that an infinite structure was considered in simulations, while a prototype with realistic dimensions ($12.5\,\text{cm} \times 12.5\,\text{cm}$) was characterized experimentally, thus favoring the discrepancies between simulation and experiment. The large level of
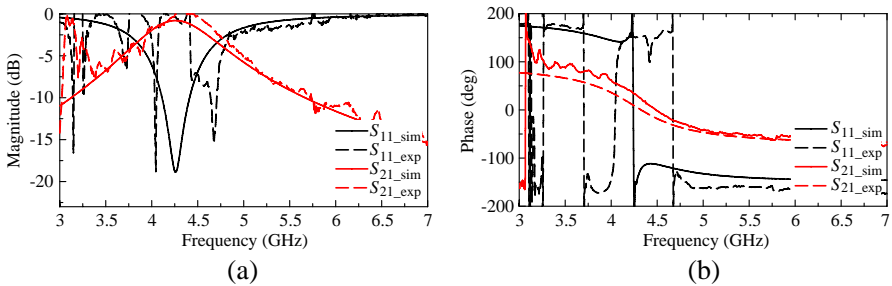

Figure 2. Calculated (solid lines) and measured (dashed lines), (a) magnitudes and (b) phases of transmission and reflection coefficients.

reflection exhibited by the metasurface beyond the resonant frequency (see Fig. 2(a)) is a key parameter for improving the directivity of printed patch antenna. Indeed, a high level of reflection is required (R should be as close as possible to unity) in order to confine electromagnetic waves in the cavity. This confinement allows achieving high directivity antenna with narrow beam, since the expression of the maximum boresight directivity is given by $D_{\max} = (1 + R)/(1 - R)$ [4].

3. DIRECTIVITY ENHANCEMENT

Following our investigations on the metasurface in the above section, we now propose to evaluate the studied metasurface as a Partially Reflecting Surface (PRS) in a FP cavity in order to enhance the directivity of a printed patch antenna. A typical cavity antenna is formed by placing a feeding source between two reflectors as shown in Fig. 3(a). For our convenience, one of the two reflectors is a PEC surface so as to prevent undesired backward radiation. The second reflector must present a high reflectivity to act as the so-called Partially Reflecting Surface (PRS) to confine the electromagnetic waves in the cavity. We then used our investigated metasurface for this purpose. From the return loss spectrum shown in Fig. 3(b), we can see a clear deep around 5.85 GHz corresponding to the resonance mode of the patch antenna, acting as the primary source of the FP cavity. A good agreement is reported between simulation and experiment. One can see that the simulated resonant frequency of the FP cavity is located at about 5.93 GHz, when the measured one falls at 5.8 GHz. This minor shift is probably due to imperfections during the fabrication process. Both the patch antenna and the FP cavity exhibit a good impedance matching (return loss < -10 dB), in the so-called 5.8 GHz band (see the shaded area in Fig. 3(b)).

The reflection phase shown in Fig. 2(b) varies from $+180°$ to $-180°$ and passes through zero at resonance. The reflection phase values are used to calculate the thickness h_r versus frequency at which maximum boresight directivity ($\theta = 0°$) can be obtained. This resonance thickness is determined by the following equation:

$$h_r = (\varphi_{PRS} + \varphi_r)\frac{\lambda}{4\pi} - t\sqrt{\varepsilon_r} \pm N\frac{\lambda}{2} \qquad (1)$$

where φ_{PRS} represents the reflection phase of the partially reflecting surface, φ_r the reflection phase of the reflector screen near the antenna, λ the operating wavelength, and N an integer corresponding to the order of the cavity's electromagnetic mode. t and ε_r are the thickness and relative dielectric permittivity of the dielectric substrate supporting the feeding source, respectively. At 5.8 GHz, a

reflection phase close $-180°$ is observed, suggesting a cavity thickness close to $\lambda/2$ (~26 mm). We shall note that the reflection at this frequency is quite high (about -1 dB), which is necessary for confining electromagnetic waves in the cavity. To illustrate the directivity enhancement, we performed numerical simulations and measurements on the cavity using the metasurface reflector. The cavity is fed by
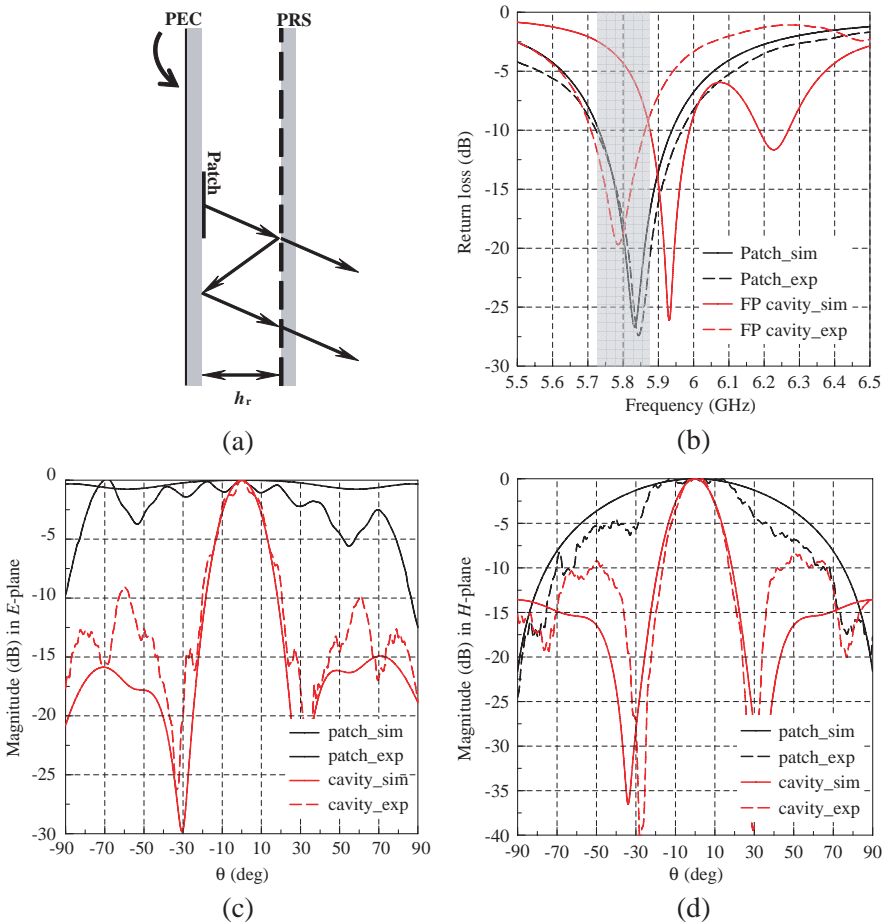

(a)

(b)

(c)

(d)

Figure 3. (a) Schematic of the metasurface-based FP cavity antenna. (b) Simulated (solid lines) and measured (dashed lines) return loss of the patch antenna acting as a primary source, and the FP cavity. The shaded area corresponds to the so-called 5.8 GHz frequency band (5.725–5.875 GHz). Calculated (solid lines) and measured (dashed lines) radiation patterns for (c) E-plane and (d) H-plane for both patch antenna and Fabry-Pérot cavity.

a microstrip patch antenna patterned also on an epoxy substrate. Figs. 3(c)–(d) show the calculated and the measured radiation patterns in E- and H-planes for the patch feed source and for the resonant FP cavity, respectively.

The performances obtained from measurements carried out on the fabricated prototypes agree very well with the numerical. The directivity of our investigated system is considerably enhanced and goes from 6 dBi for the patch antenna to about 18 dBi for the cavity and the parasitic side lobes level of the cavity remains below -10 dB. These results show the potential application of our proposed metasurface in a FP cavity for highly directive emissions.

4. APPLICATION OF THE FABRY-PEROT CAVITY ANTENNA IN A CONTACTLESS BREATHING SENSOR

The block diagram of the implemented respiratory monitoring system is depicted in Fig. 4. Assume a monochromatic signal $x(t)$, generated
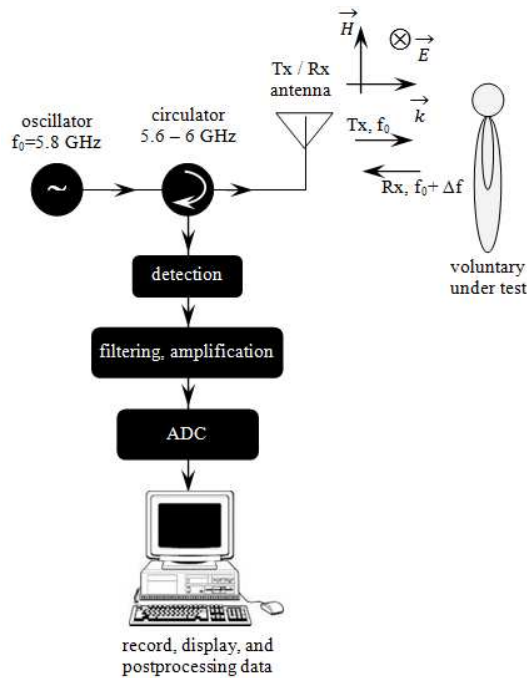

Figure 4. Block diagram of our proposed monochromatic wave radar-based respiration sensor including the investigated FP cavity antenna. The polarization of the incident electric field E, magnetic field H, and wave vector k are illustrated in the figure.

by an oscillator, and given by the following expression:

$$x(t) = A\cos(2\pi f_0 t) \tag{2}$$

where A designates the amplitude of the signal, f_0 designates the operating frequency, which is set to 5.8 GHz. The choice of this frequency is pushed by the necessity to belong to the ISM band (Industrial Scientific and Medical). Furthermore, the 5.8 GHz band is a well known communication standard, limited by an equivalent isotropically radiated power EIRP of 200 mW (i.e., 23 dBm) for an exclusively indoor use. EIRP is a standard, to which must satisfy the ISM equipments, in order to minimize the human-being exposure to electromagnetic field. Its expression is given as follows:

$$\text{EIRP}\,[\text{dBm}] = P_T\,[\text{dBm}] - L_C\,[\text{dB}] + G_a\,[\text{dBi}] \tag{3}$$

in which P_T designates the output power of the transmitter, L_c designates the cable losses, and G_a designates the antenna gain. The transmitter channel through which the generated signal flows before being radiated by the transmitting antenna is composed of: an oscillator, a narrow-band circulator operating in the 5.6–6 GHz frequency range, and a transmitting antenna. The radiated electromagnetic waves are scattered by the target (voluntary under test). The movement of the patient's chest caused by the respiration and heart beat leads to variations of the frequency of the scattered signal, owing to Doppler-Effect. The reflected signal will include the frequency of the transmitted signal provided by the generator f_0, with a frequency shift Δf, which is proportional to the displacement velocity of the target, (e.g., the patient's thorax). The received signal, carrying the desired information (i.e., the frequency of respiration Δf) is therefore expressed as follows:

$$y(t) = B\cos[(\omega_0 + \Delta\omega)t] \tag{4}$$

where,

$$\Delta\omega = 2v\omega_0/c$$

in which B designates the amplitude of the received signal, ω_0 the working frequency, v the velocity of the moving target under test, and c the speed of light. The received signal is collected by the same antenna, which also acts as a receiving antenna (we focused on a monostatic approach), and is derived towards the receive channel via the narrow-band circulator (5.6–6 GHz). Note that the standard technique of measure involving a splitter and a frequency mixer is replaced in this present work by a much more compact approach, thus favoring the integration process. Indeed, the detection of the amplitude of the refracted signal is performed by a Schottky diode-based system, thus

giving rise to a DC voltage proportional to the displacement velocity of the target. The output signal is then filtered, amplified, and recorded in a computer memory through an interface module (analog to digital conversion system). The measured gain of the FP cavity antenna at 5.8 GHz is about 18 dBi. The nominal power of the oscillator is then set to about 5 dBm (∼3 mW), thus limiting the PIRE to an authorized value of 23 dBm (200 mW).

The breathing sensor was tested on a person lying on his back, placed at about 1.5 m from the antenna. The result of the breath record over a time window of about 30 s is represented in the inset of Fig. 5. The frequency spectrum of the breath record is shown in Fig. 5. The result of the spectral analysis using Fast Fourier Transform (FFT) reveals a pronounced peak around 0.2 Hz (denoted by an arrow), which corresponds to a frequency of respiration of 12 cycles/min (adult at rest). Further records (not represented here) demonstrate the ability of the sensor to detect precisely temporal signatures resulting from the breathing activity, and those due to gestural movements of the voluntary under-test.
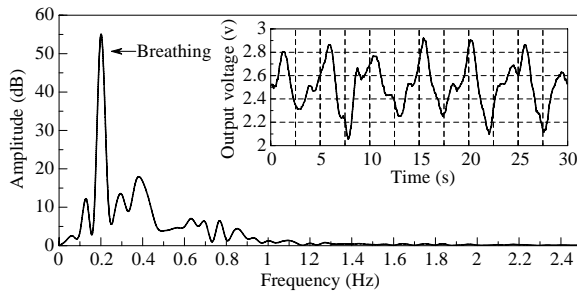

Figure 5. Frequency spectrum of the recorded breathing signal presented in the inset, over a time window of about 30 s. The frequency of respiration is estimated at about 0.2 Hz (denoted by an arrow).

5. CONCLUSION

In summary, we have numerically and experimentally investigated a planar metasurface that has been designed, fabricated and characterized for an operation frequency in the microwave regime. The investigated metasurface has been used as a Partially Reflecting Surface in a Fabry-Pérot cavity where the radiation patterns have shown a highly directive emission. The proposed FP cavity antenna was embedded in a contactless breathing sensor based on the principle

of monochromatic wave radar. Experimental measurements carried out on a voluntary-under-test have demonstrated successfully the feasability of a remote sensing vital signs. This is a very promising step to provide health care facilities with compact, low-cost, and non-invasive respiration sensors.

ACKNOWLEDGMENT

REFERENCES

1. Lin, J. C., J. Kiernicki, M. Kiernicki, and P. B. Wollschlaeger, "Microwave apexcardiography," *IEEE Trans. Microw. Theory Tech.*, Vol. 27, No. 6, 618–620, 1979.

2. Matsui, T., H. Hattori, B. Takase, and M. Ishihara, "Non-invasive estimation of arterial blood pH using exhaled CO/CO_2 analyzer microwave radar and infrared thermography for patients after massive hemorrhage," *Journal of Medical Engineering and Technology*, Vol. 20, No. 2, 97–101, 2006.

3. Trentini, G. V., "Partially reflecting sheet array," *IRE Trans. Antennas Propag.*, Vol. 4, No. 4, 666–671, 1956.

4. Feresidis, A. P., G. Goussetis, S. Wang, and J. C. Vardaxoglou, "Artificial magnetic conductor surfaces and their application to low-profile high-gain planar antennas," *IEEE Trans. Antennas Propag.*, Vol. 53, No. 1, 209–215, 2005.

5. Zhou, L., H. Li, Y. Qin, Z. Wei, and C. T. Chan, "Directive emissions from subwavelength metamaterial-based cavities," *Appl. Phys. Lett.*, Vol. 86, No. 10, 101101-1–101101-3, 2005.

6. Ourir, A., A. de Lustrac, and J.-M. Lourtioz, "All-metamaterial-based sub-wavelength cavities ($\lambda/60$) for ultrathin directive antennas," *Appl. Phys. Lett.*, Vol. 88, No. 8, 084103-1–084103-3, 2006.

7. Yahiaoui, R., S. N. Burokur, and A. de Lustrac, "Enhanced directivity of ultra-thin metamaterial-based cavity antenna fed by multisource," *Electron. Lett.*, Vol. 45, No. 16, 814–816, 2009.

8. Burokur, S. N., R. Yahiaoui, and A. de Lustrac, "Subwavelength metamaterial-based resonant cavities fed by multiple sources for high directivity," *Microwave Opt. Technol. Lett.*, Vol. 51, No. 8, 1883–1888, 2009.

9. Burokur, S. N., J.-P. Daniel, P. Ratajczak, and A. de Lustrac, "Tunable bilayered metasurface for frequency reconfigurable directive emissions," *Appl. Phys. Lett.*, Vol. 97, No. 6, 064101-1–064101-3, 2010.

10. Yahiaoui, R., S. N. Burokur, V. Vigneras, A. de Lustrac, and P. Mounaix, "Investigation of spatial filters at microwave frequencies: Application for antenna directivity enhancement," *Microwave Opt. Technol. Lett.*, Vol. 54, No. 5, 1327–1332, 2012.